Physica B 407 (2012) 4081–4085

Contents lists available at SciVerse ScienceDirect

Physica B

journal homepage: www.elsevier.com/locate/physb

Collective resonances in plasmonic crystals: Size matters

S.R.K. Rodriguez [a,1], M.C. Schaafsma [a,1], A. Berrier [a], J. Gómez Rivas [a,b,*]

[a] Center for Nanophotonics, FOM Institute AMOLF, c/o Philips Research Laboratories, High Tech Campus 4, 5656 AE Eindhoven, The Netherlands
[b] COBRA Research Institute, Eindhoven University of Technology, P.O. Box 513, 5600 MB Eindhoven, The Netherlands

ARTICLE INFO

Available online 27 March 2012

Keywords:
Surface plasmon polaritons
Surface lattice resonances
Metallic nanoparticles
Coupled dipole model
Diffraction

ABSTRACT

Periodic arrays of metallic nanoparticles may sustain surface lattice resonances (SLRs), which are collective resonances associated with the diffractive coupling of localized surface plasmons resonances (LSPRs). By investigating a series of arrays with varying number of particles, we traced the evolution of SLRs to its origins. Polarization resolved extinction spectra of arrays formed by a few nanoparticles were measured, and found to be in very good agreement with calculations based on a coupled dipole model. Finite size effects on the optical properties of the arrays are observed, and our results provide insight into the characteristic length scales for collective plasmonic effects: for arrays smaller than $\sim 5 \times 5$ particles, the *Q*-factors of SLRs are lower than those of LSPRs; for arrays larger than $\sim 20 \times 20$ particles, the *Q*-factors of SLRs saturate at a much larger value than those of LSPRs; in between, the *Q*-factors of SLRs are an increasing function of the number of particles in the array.

1. Introduction

Sophisticated methods for manipulating light at the nanoscale are increasingly developed in the field of metallic nano-optics [1]. Although metals may provide advantages over dielectrics associated with the large electromagnetic enhancements they may create [2], the high losses accompanying resonant effects pose a serious challenge for their emergence as a viable technology [3]. The development of resonances with high quality factor *Q* is therefore of great relevance in the field of nanoplasmonics. One way to minimize losses in plasmonic systems is based on collective resonances [4], which leads to a modification of radiative damping—the dominant contribution to the plasmon linewidth. In the case of periodic arrays of metallic nanoparticles, it was calculated that near the critical energy where a diffraction order changes from radiating to evanescent in character, dipolar interactions would lead to the emergence of a new, narrow linewidth plasmonic resonance [5].

Carron et al. seem to have been the first to investigate this phenomenon experimentally [6], but the resonances were not as sharp as predicted by the theory due to technological limitations rendering imperfect structures. Schatz, Zou, and co-workers revived the interest in these lattice-induced plasmonic resonances with a series of theoretical papers mainly based on the coupled dipole model (CDM). Extinction efficiencies higher than 30 were predicted [7], but experimental observation of these narrow resonances remained elusive [8]. These resonances are now known as surface lattice resonances (SLRs), and they have been observed experimentally in the recent years by several groups [9–12]. SLRs arise from the diffractive coupling of localized surface plasmon resonances (LSPRs) of individual particles. This coupling is mediated by Rayleigh anomalies, which correspond to the condition whereby a diffracted wave propagates in the plane of the array. The properties of SLRs, just as those of LSPRs, generally depend on size, geometry and composition of the particle, and on the surrounding medium and polarization of the light field [9]. Moreover, due to their collective nature, SLRs rely strongly on the interparticle distance and on the long-range order in the lattice [13]. A question that remains open is how the number of particles in the array influences the properties of SLRs. Remarkable insight into this problem has been obtained for the complementary structures of subwavelength hole arrays in metallic films [14,15]. However, the influence of finite size effects on the optical properties of nanoparticle arrays sustaining collective resonances has not been discussed yet. Although a similar response is expected for nanohole and nanoparticle arrays based on Babinet's principle [16], we highlight that there is a fundamental difference between the two systems. Namely, whereas radiative coupling in nanohole arrays may take place via surface plasmon polaritons propagating through continuous metallic films, nanoparticle arrays consist of isolated metallic islands that may electromagnetically couple through diffraction.

In this paper, we present an experimental and theoretical study on the evolution of SLRs as a function of the number of particles in the array. We investigate finite size effects on the

* Corresponding author at: Center for Nanophotonics, FOM Institute AMOLF, c/o Philips Research Laboratories, High Tech Campus 4, 5656 AE Eindhoven, The Netherlands. Tel.: +31 402742349; fax: +31 402746505.
E-mail address: rivas@amolf.nl (J. Gómez Rivas).
[1] These authors had an equal contribution.

0921-4526/$ - see front matter © 2012 Elsevier B.V. All rights reserved.
http://dx.doi.org/10.1016/j.physb.2012.03.053

extinction spectra starting at the smallest array size, i.e., 2×2 particles. This work is organized as follows. In Section 2 we describe the samples and experimental methods. In Section 3 we provide an overview of the coupled dipole model (CDM), which we use to calculate the extinction spectra of various arrays. In Section 4 we compare the measurements to the CDM calculations.

2. Sample and experimental methods

A series of gold nanodisk arrays with dimensions of $N\times N$ particles, N ranging from 2 to 10, were fabricated by electron beam lithography onto an amorphous quartz substrate. The nanodisks have a height of 50 nm, a diameter of 120 nm, and they are arranged in rectangular arrays with lattice constants $a_x=500$ nm and $a_y=300$ nm. In order to surround the arrays by a homogeneous medium, we evaporated 150 nm of silica on top, added index matching fluid of $n=1.45$, and placed an amorphous quartz superstrate identical to the substrate. The homogeneous environment was created in order to enhance the diffractive coupling of the particles [16].

A confocal microscope with a two-axis translation stage with a precision of 200 nm was used for the extinction experiments. A white light beam from a halogen lamp impinged from below onto the samples at normal incidence, rendering a plane wave excitation. The transmitted light was collected by the microscope's objective and directed into a fiber coupled spectrophotometer. The polarization of the incident light was set parallel to the $a_y=300$ nm pitch, so that diffractive coupling along the $a_x=500$ nm may take place. In order to detect the full extinction of the incident plane wave, the angle subtended by the detector should be sufficiently small [17]. This translates into the requirement for a small numerical aperture (NA) and a small aperture of the confocal pinhole in the collection path, which poses a challenge for detecting the low signals produced in extinction by small arrays. We used a $20\times$, NA=0.4 objective, and a 60 μm confocal pinhole, which represents an improvement relative to studies with a higher NA's [10]. The field of view (FoV) seen by the detector was determined by the knife-edge technique, in which the transmitted power is measured across the boundary between a transparent surface and a metallic layer; we found a FoV $=6.0\pm 0.5$ μm.

3. Theory

The coupled dipole method (CDM) under the modified long wavelength approximation (MLWA) is widely used for calculating extinction spectra of nanoparticle arrays [18,7]. The CDM is based on modeling each particle as a radiating dipole, and calculating its interaction with the fields radiated by all other dipoles in the array. We herein provide an overview of the CDM.

3.1. Polarizability of a single particle

Since no closed-form solution exists for the polarizability of cylinders, the nanodisks are approximated as oblate spheroids [19]. The static polarizability of an ellipsoid along one of its main axes is given by

$$\alpha^{static}=\frac{(\epsilon_p-\epsilon_d)}{[3(\epsilon_p-\epsilon_d)\cdot L+3\epsilon_d]}\cdot V, \tag{1}$$

with ϵ_p and ϵ_d the relative dielectric constants of the particle and of the surrounding dielectric, respectively, V the volume of the particle, and L a form factor for each of the three main axes of the ellipsoid [20]. In the MLWA, the static polarizability is modified to account for dynamic depolarization and radiative damping. This polarizability is given by

$$\alpha=\frac{\alpha^{static}}{1-\frac{2}{3}ik^3\alpha^{static}-\frac{k^2}{r}\alpha^{static}}, \tag{2}$$

where $k=2\pi n/\lambda$ is the incident wave vector with λ the vacuum wavelength and n the refractive index of the surrounding dielectric, and r is the radius of the main axis of the ellipsoid in the direction of the polarization. The term $\frac{2}{3}ik^3\alpha^{static}$ corresponds to dynamic depolarization, and the term $(k^2/r)\alpha^{static}$ accounts for radiative damping [18].

3.2. Coupled dipole model (CDM)

From the polarizability α_i at position r_i of the array, the polarization of the medium P_i can be calculated with the relation $P_i=\alpha_i E_{loc,i}$, where $E_{loc,i}$ is the local field, given by the sum of the incident field and the fields scattered by all other particles. Under plane wave illumination, the local field can be expressed as

$$E_{loc,i}=E_0e^{ikr_i}-\sum_{\substack{j=1\\ j\neq i}}^{N^2}A_{ij}\cdot P_j, \tag{3}$$

where A_{ij} represents the dipolar interaction between particles i and j, and its dot product with P_j reads

$$A_{ij}\cdot P_j=k^2e^{ikr_{ij}}\frac{r_{ij}\times(r_{ij}\times P_j)}{r_{ij}^3}+e^{ikr_{ij}}(1-ikr_{ij})\frac{r_{ij}^3P_j-3r_{ij}(r_{ij}\cdot P_j)}{r_{ij}^5}\quad (i,j=1\ldots N^2,\ i\neq j) \tag{4}$$

for an $N\times N$ particle array. The polarization vector $\tilde{P}$ can be calculated from

$$\tilde{E}=\tilde{\tilde{A}}'\tilde{P}, \tag{5}$$

where the diagonal terms of $\tilde{\tilde{A}}'$ are $A_{ii}=\alpha_i^{-1}$, and the off-diagonal terms of $\tilde{\tilde{A}}'$ are calculated from Eq. (4). From the polarization vectors, the extinction cross section of the array can be calculated using

$$C_{ext}=\frac{4\pi k}{|E_0|^2}\sum_{i=1}^{N^2}Im(E_{inc,i}^*\cdot P_i), \tag{6}$$

where $E_{inc,i}^*$ is the complex conjugate of the incident field [17]. An extinction efficiency η_{ext} can be obtained by normalizing the extinction of the array to the sum of the geometrical cross section of the particles, i.e.,

$$\eta_{ext}=\frac{C_{ext}}{N^2A_p}, \tag{7}$$

with A_p the cross sectional area of each particle.

In order to compare theoretical extinction spectra with experimental transmittance spectra, we define the *Extinction* $=1-T$, with T the transmittance in the forward direction within the NA of the objective. To obtain a transmittance from Eq. (6) that may result in quantitative agreement with experimental data, the *FoV* in the experiments needs to be considered. In our case, the *FoV* is equal for all arrays, and larger than the largest array. This leads to a transmittance given by

$$T=1-\frac{C_{ext}}{FoV}. \tag{8}$$

Although the focus of the present work is on finite size effects in nanoparticle arrays, it is instructive to assess how well the response of very large, but finite, arrays converges to the response of an 'infinite' array. For 'infinite' arrays illuminated at normal incidence, Eq. (5) can be simplified assuming that the induced

polarization in all particles is equal. This leads to an effective polarizability $\alpha^{\star}$, given by [7]

$$\alpha^{\star} = \frac{1}{1/\alpha - S}, \tag{9}$$

where S is the retarded dipole sum given by

$$S = \sum_{j \neq i} \frac{(1-ikr_{ij})(3\cos^2\theta_{ij}-1)e^{ikr_{ij}}}{r_{ij}^3} + \frac{k^2 \sin^2\theta_{ij} e^{ikr_{ij}}}{r_{ij}}, \tag{10}$$

with θ_{ij} the angle between r_{ij} and the polarization direction. Note that S is a purely geometrical factor through which the lattice modifies the polarizabilities of the individual particles, so that when $1/\alpha = S$ a pole in $\alpha^{\star}$ occurs, giving rise to a lattice-induced resonance. Because α and S are in general complex numbers, strict equality does not occur and $\alpha^{\star}$ remains finite. However, a resonance indeed arises when the real part of $1/\alpha - S$ vanishes.

4. Results

Fig. 1 shows extinction spectra as obtained from measurements (a), and CDM calculations (b), for the arrays described in Section 2. At $\lambda \approx 780$ nm we observe a peak gradually growing in extinction as the array size increases. This peak is the SLR, becoming increasingly sharper due to a collective suppression of radiative damping. The local minimum seen in extinction at $\lambda \approx 745$ nm corresponds to the Rayleigh anomaly. We also note a secondary maximum in extinction observed at $\lambda \approx 720$ nm. Félidj et al., observed a similar feature which, together with the primary resonance, they attributed to two diffracted waves into different media [21]. However, the observation of a very similar feature by Auguié and Barnes in a fully homogeneous medium [9] questioned the explanation provided by Félidj et al. At this point, we would like to clarify that to obtain the good agreement between measurements and calculations seen in Fig. 1, we did not use normally incident illumination alone. Instead, the spectra in Fig. 1(b) were calculated by averaging the extinction over angles of incidence between $\theta = 0^{\circ}$ and 6°. This implies that the incident beam in the experiment was not well collimated. The motivation to angularly average the extinction spectra, and its connection with the secondary minimum seen in Refs. [9,21], is discussed next.

Fig. 2(a) shows the calculated variable angle extinction efficiency spectra for an array of 10×10 particles. Two sharp resonances are

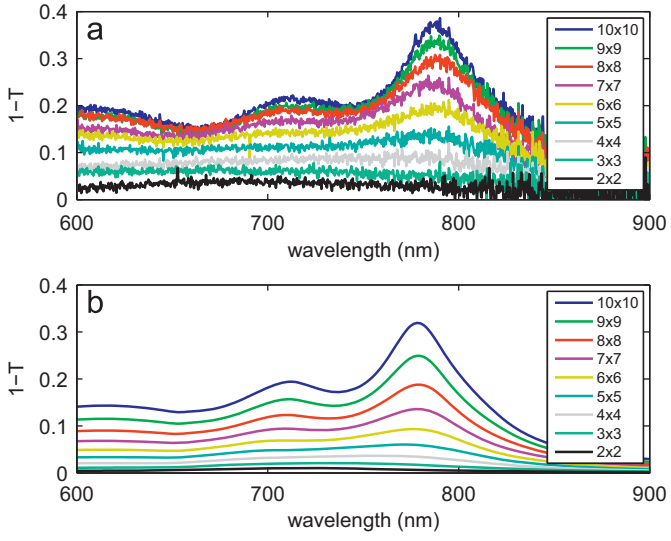

Fig. 1. (a) Measurements and (b) coupled dipole model calculations of the extinction spectra of $N \times N$ gold nanodisk arrays, where N ranges from 2 to 10.

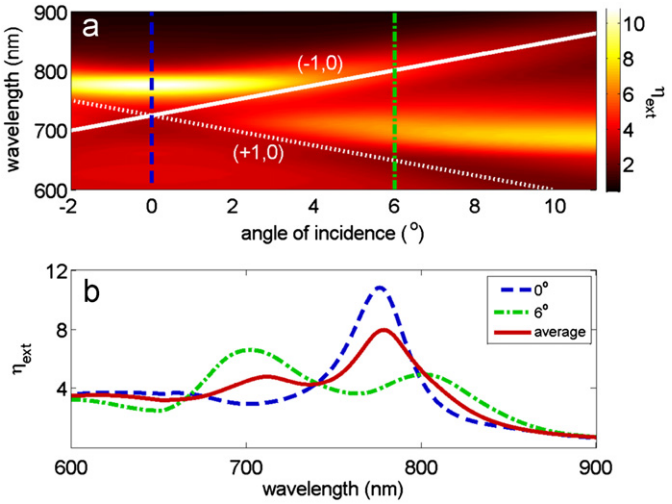

Fig. 2. Coupled dipole model calculations for an array of 10×10 gold nanodisks. (a) Variable angle extinction spectra and (b) the dashed and dashed–dotted curves are cuts at $\theta = 0^{\circ}$ and $\theta = 6^{\circ}$ of (a), respectively, and the solid curve is the average extinction between 0° and 6°.

seen in the spectra, displaying an anti-crossing behavior near normal incidence associated with their mutual coupling. The peak in extinction at $\lambda \approx 780$ nm and $\theta = 0^{\circ}$ is the SLR associated with the $(-1,0)$ diffraction order – this is the primary peak in the spectra of Fig. 1(b). The peak in extinction at $\lambda \approx 700$ nm and $\theta = 6^{\circ}$ is the $(+1,0)$ SLR – this is the secondary peak in extinction. Thus, we observe that the coupling between the $(+1,0)$ and $(-1,0)$ SLRs leads to the opening of a stop-gap in the dispersion relation of the array. The mutual coupling between bright and dark SLRs (in 'infinite' arrays) and the consequent opening of the gap were recently discussed [22]. By bright/dark it is meant that the resonance couples efficiently/inefficiently to light, which results from a symmetric/antisymmetric field distribution. Notice that only for angles of incidence of $\theta \gtrsim 2^{\circ}$, the $(-1,0)$ SLR center wavelength increases with the angle. The flattening of the band observed near normal incidence indicates a reduction of the mode's group velocity and the formation of standing waves. This is the origin of the high extinction from the $(-1,0)$ SLR at normal incidence, since the density of optical states is enhanced at the band-edge. On the other hand, the $(+1,0)$ SLR cannot be excited by a normally incident plane wave; a narrowing of the plasmon linewidth and a diminishing extinction are seen as the angle of incidence approaches $\theta = 0^{\circ}$. The observed behavior is characteristic of subradiant damping, whereby radiative damping is suppressed due to antisymmetric field distributions [4]. In Fig. 2(b) we display cuts in angle at $\theta = 0^{\circ}$, $\theta = 6^{\circ}$ of Fig. 2(a), and average the spectra between $\theta = 0^{\circ}$ and $\theta = 6^{\circ}$. By comparing the three curves in Fig. 2(b) with the experimental data in Fig. 1(a) for the 10×10 array, it is clear that the best agreement between measurements and calculations is obtained by assuming that the incident beam contains a distribution of k-vectors, which on a best-fit basis, we estimated to include angles of up to 6°. Therefore, the variable angle extinction spectra in Fig. 2 explain the features we observe in the experiments, and also elucidate what is most likely the origin of the secondary peak in extinction seen in Refs. [9,21], and also in other studies [11], i.e., a non-perfectly collimated incident beam.

As observed in Fig. 2 and discussed in Ref. [22], SLRs are Fano resonances [23], i.e., asymmetric resonances molded by the interference between two channels: the scattered intensity in the plane of the array at the Rayleigh anomaly condition, and the background transmission. Although Fano described quantum interference phenomena, his model has found broad applicability to classical systems also, and particularly in plasmonics [24,25].

We have fitted the extinction efficiency spectra for each array with a Fano equation of the form

$$\eta_{eff} = C_0 \frac{[q+2(\omega-\omega_0)/\Gamma]^2}{1+[2(\omega-\omega_0)/\Gamma]^2}, \tag{11}$$

with C_0 an amplitude constant, ω_0 the resonance center frequency, and Γ the linewidth [26]. From the fitted values, we have calculated a quality factor $Q_{SLR}=\omega_0/\Gamma$, which is shown in Fig. 3(a) as a function of the number of particles N along each dimension of the array. This expression for the quality factor defines the ratio of the stored to dissipated energy only in Lorentzian resonators. Nevertheless, we use it to characterize the spectral narrowing and to obtain a qualitative insight into the suppression of radiative damping as the size of the array increases. For comparison, we plot as horizontal lines in Fig. 3(a) the calculated Q of a single particle, Q_s, and of an 'infinite' array, Q_∞. In Fig. 3(b) we show the extinction spectra for some of the finite arrays to illustrate how the SLR lineshapes evolve as N increases. In Fig. 3(c) we show the single particle and 'infinite' array spectra; the latter was calculated using Eqs. (9) and (10). Fig. 3 shows how the increasing extinction at the SLR wavelength and the simultaneous spectral narrowing lead to an increasing Q_{SLR}.

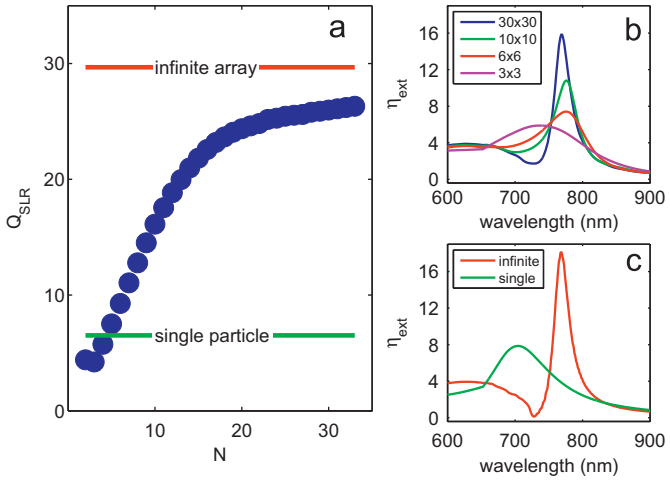

Fig. 3. (a) Calculated quality factor of SLRs (Q_{SLR}) as a function of the number of particles (N) along each dimension of the array. (b) Calculated extinction spectra for some of the arrays yielding the increasing Q_{SLR} in (a). (c) Calculated extinction spectra of a single particle and an infinite array. The quality factors of the single particle and the infinite array are indicated by the horizontal lines in (a).

From the values reported in Fig. 3(a), we may identify three regimes for Q_{SLR}: (i) for $N<5$, $Q_{SLR}<Q_s$; (ii) for $5<N<20$, Q_{SLR} increases rapidly; and (iii) for $N>20$, Q_{SLR} begins to saturate, slowly approaching the value $Q_\infty \approx 30$ of the 'infinite' array. We understand the evolution of Q_{SLR} through the three regimes as follows. In the first regime, collective effects are weak. The extinction displays several peaks of similar magnitude which together yield a 'linewidth' significantly broader than that of the single particle resonance. The weak collective behavior is due to the large fraction of particles located at the edges of the array. Although this regime was neither measured nor identified in Ref. [27], the authors discussed the underlying mechanism by which a decreasing array size leads to a reduction in Q for a collective resonance: scattering losses at the edges of the array. In the second regime, the fraction of particles at the edges decreases and the number of particles resonating collectively increases, which lead to a rapid increase in Q_{SLR}. In the third regime, further addition of particles to the array does not affect drastically Q_{SLR}. Although the in plane scattering losses continue to diminish, the out-of plane scattering losses and material losses become the dominant contribution to the linewidth. This can be intuitively understood by considering the propagation lengths for the surface polaritons associated with SLRs. In Ref. [28], propagation lengths on the order of $\sim 10\,\mu m$ were found for similar arrays of gold nanoparticles. In the present work, diffractive coupling takes place along the $a_x=500$ nm pitch of the structure, which means that 10 μm corresponds to 20 unit cells. Not coincidentally, Q_{SLR} begins to saturate near $N=20$. Since further addition of particles does not contribute significantly to the extinction, the arrays become effectively 'infinite'.

Fig. 4 shows results from finite element method (FEM) simulations (COMSOL) for an 'infinite' array of nanodisks as those in the measurements and CDM calculations. Periodic boundary conditions

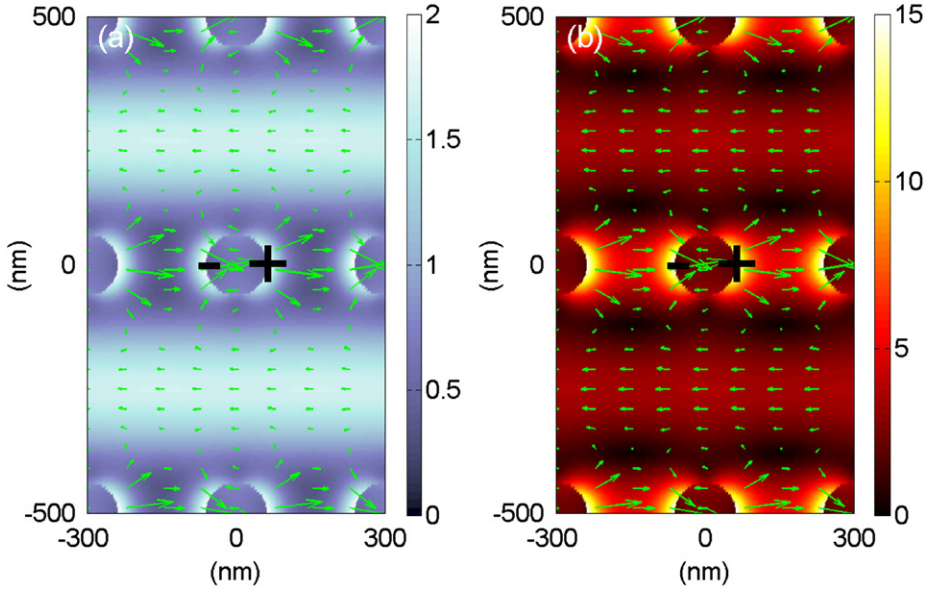

Fig. 4. Total field enhancement (color scales) and scattered field (arrows) for an infinite array of gold nanodisks surrounded by amorphous quartz. Both plots are at a plane intersecting the nanodisks at their midheight. The illumination is a normally incident plane wave with a vacuum wavelength of (a) $\lambda=670$ nm and (b) $\lambda=780$ nm, which corresponds to the wavelengths of the LSPR and SLR, respectively. The polarization vector is along the same axis as the excited dipole moment in the individual particles, indicated by the + and − signs. (For interpretation of the references to color in this figure legend, the reader is referred to the web version of this article.)

were used, and the particles are illuminated by a normally incident plane wave. The transmittance spectra was first calculated, and it was found to be in excellent agreement with the 'infinite' array spectra obtained from the CDM (Fig. 3(c)). In Fig. 4, we present the field enhancement (in color scale) and the scattered field (arrows) at a plane intersecting the particles at their midheight, for two values of the vacuum wavelength. Fig. 4(a) shows the spectra at $\lambda = 670$ nm, which corresponds to the broad and weak feature seen in extinction. As it can be recognized from the field pattern, a dipolar resonance is excited in the individual particles. A small field enhancement is observed near the surface of the particles, but the region in between the particles exhibits field suppression. The particles are therefore individually resonant with the incident field and there is no collective behavior. This is the typical behavior of LSPRs. In Fig. 4(b) we show the fields at $\lambda = 780$ nm, which corresponds to the SLR wavelength. Notice that a dipolar resonance is excited as well, having an almost identical radiation pattern to that in Fig. 4(a), but with two important differences: the field enhancements are much larger (almost by an order of magnitude), and the scattered intensity in the area between the particles is much higher. This has important consequences for applications in sensing and modified spontaneous emission where molecules may profit from a high density of states over extended volumes.

In conclusion, we have demonstrated finite size effects in the optical properties of metallic nanoparticle arrays. The critical length scales over which collective effects are important were discussed. We have identified an array size-dependent quality factor for surface lattice resonances arising from the diffractive coupling of localized surface plasmons (Q_{SLR}). Q_{SLR} is lower than the Q of the single particle resonance for arrays smaller than 5×5 particles. For arrays sizes between 5×5 and 20×20 particles, Q_{SLR} dramatically increases beyond the value of Q_s, saturating for larger arrays.

Acknowledgments

We would like to thank Costas Soukoulis for his truly inspiring scientific works and conferences that have had a deep impact in a whole generation of nanophotonics researchers. We would like to acknowledge Bas Ketelaars for assistance in the fabrication of the samples. This work was supported by the Netherlands Foundation Fundamenteel Onderzoek der Materie (FOM) and the Nederlandse Organisatie voor Wetenschappelijk Onderzoek (NWO), and is part of an industrial partnership program between Philips and FOM.

References

[1] C. Soukoulis, M. Wegener, Nat. Photonics 5 (2011) 523.
[2] J. Aizpurua, G.W. Bryant, L.J. Richter, F.J. García de Abajo, B.K. Kelley, T. Mallouk, Phys. Rev. B 71 (2005) 235420.
[3] C. Soukoulis, M. Wegener, Science 330 (2010) 1633.
[4] C. Ropers, D.J. Park, G. Stibenz, G. Steinmeyer, J. Kim, D.S. Kim, C. Lienau, Phys. Rev. Lett. 94 (2005) 113901.
[5] M. Meier, A. Wokayn, P. Liao, J. Opt. Soc. Am. B 2 (1985) 931.
[6] K.T. Carron, W. Fluhr, M. Meier, A. Wokaun, H.W. Lehmann, J. Opt. Soc. Am. B 3 (1986) 430.
[7] S. Zou, N. Janel, G. Schatz, J. Phys. Chem. B 120 (2004) 10871.
[8] E.M. Hicks, S. Zou, G.C. Schatz, K.G. Spears, R.P. Van Duyne, L. Gunnarsson, T. Rindzevicius, B. Kasemo, M. Käll, Nano Lett. 5 (2005) 1065.
[9] B. Auguié, W.L. Barnes, Phys. Rev. Lett. 101 (2008) 143902.
[10] Y. Chu, E. Schonbrun, T. Yang, K.B. Crozier, Appl. Phys. Lett. 93 (2008) 181108.
[11] V.G. Kravets, F. Schedin, A.N. Grigorenko, Phys. Rev. Lett. 101 (2008) 087403.
[12] G. Vecchi, G. Giannini, J. Gomez-Rivas, Phys. Rev. Lett. 102 (2009) 146807.
[13] B. Auguié, W.L. Barnes, Opt. Lett. 34 (2009) 401.
[14] J. Bravo-Abad, A. Degiron, F. Przybilla, C. Genet, F. Garcia-Vidal, L. Martin-Moreno, T. Ebbesen, Nat. Phys. 2 (2006) 120.
[15] F. Przybilla, A. Degiron, C. Genet, T. Ebbesen, F. de Leon-Perez, J. Bravo-Abad, F. Garcia-Vidal, L. Martin-Moreno, Opt. Express 16 (2008) 9571.
[16] B. Auguié, X.M. Bendaña, W.L. Barnes, F.J. Garcia de Abajo, Phys. Rev. B 82 (2010) 155447.
[17] C.F. Bohren, D.R. Huffman, Absorption and Scattering of Light by Small Particles, first ed., John Wiley Sons, Inc., New York, 1983.
[18] T. Jensen, L. Kelly, A. Lazarides, G. Schatz, J. Cluster Sci. 10 (1999) 295.
[19] J. Venermo, A. Sihvola, J. Electrostatics 63 (2005) 101.
[20] H. de Hulst, Light Scattering by Small Particles, first ed., Dover, New York, 1981.
[21] N. Felidj, G. Laurent, J. Aubard, G. Levi, A. Hohenau, J. Kremm, F.R. Aussenegg, J. Chem. Phys. 123 (2005) 221103.
[22] S.R.K. Rodriguez, A. Abass, B. Maes, O.T.A. Janssen, G. Vecchi, J. Gómez Rivas, Phys. Rev. X 1 (2011) 021019.
[23] U. Fano, Phys. Rev. 124 (1961) 1866.
[24] C. Genet, M.P. van Exter, J.P. Woerdman, Opt. Commun. 225 (2003) 331.
[25] B. Luk'yanchuk, N.I. Zheludev, S.A. Maier, N.J. Halas, P. Nordlander, H. Giessen, C.T. Chong, Nat. Mater. 9 (2010) 707.
[26] M. Galli, S.L. Portalupi, M. Belotti, L.C. Andreani, L. O'Faolain, T.F. Krauss, Appl. Phys. Lett. 94 (2009) 071101.
[27] V.A. Fedotov, N. Papasimakis, E. Plum, A. Bitzer, M. Walther, P. Kuo, D.P. Tsai, N.I. Zheludev, Phys. Rev. Lett. 104 (2010) 223901.
[28] G. Vecchi, V. Giannini, J. Gómez Rivas, Phys. Rev. B 80 (2009) 201401.